

Chapter 19

Neutrino Masses and Flavor Oscillations

Yifang Wang and Zhi-zhong Xing*

Institute of High Energy Physics, Chinese Academy of Sciences,

P.O. Box 918, Beijing 100049, China

**xingzz@ihep.ac.cn*

This essay is intended to provide a brief description of the peculiar properties of neutrinos within and beyond the standard theory of weak interactions. The focus is on the flavor oscillations of massive neutrinos, from which one has achieved some striking knowledge about their mass spectrum and flavor mixing pattern. The experimental prospects towards probing the absolute neutrino mass scale, possible Majorana nature and CP-violating effects, will also be addressed.

1. Neutrinos and Their Sources

1.1. *From Pauli's hypothesis to the discoveries of neutrinos*

Soon after Henri Becquerel discovered the radioactivity of uranium in 1896,¹ many nuclear physicists started to pay attention to the beta decays $(A, Z) \rightarrow (A, Z + 1) + e^-$, in which the energy spectrum of electrons was expected to be *discrete* thanks to the laws of energy and momentum conservations. However, James Chadwick observed a *continuous* electron energy spectrum of the beta decay in 1914,² and such a result was firmly confirmed by Charles Ellis and his colleagues in the 1920s.³ At that time there were two different ideas to resolve this “new physics” phenomenon (i.e., the discrepancy between *observed* and *expected* energy spectra of electrons): one was to give up the energy conservation law and the other was to add in a new particle. Niels Bohr was the representative of the former idea, which turned out to be wrong. Wolfgang Pauli conjectured that an unobservable, light, spin-1/2 and neutral particle — known as the electron antineutrino later — appeared in the beta decay and carried away some energy and momentum, and thus the energy spectrum of electrons in the process $(A, Z) \rightarrow (A, Z + 1) + e^- + \bar{\nu}_e$ was continuous. Pauli first put forward the concept of neutrinos in his famous letter to the “Dear radioactive ladies and gentlemen” who had gathered in Tübingen on 4 December 1930.⁴ Three years later he gave a talk on his neutrino hypothesis in the renowned Solvay Conference, where Enrico Fermi was in the audience and took

© 2016 Author(s). Open Access chapter published by World Scientific Publishing Company and distributed under the terms of the Creative Commons Attribution Non-Commerical (CC BY-NC) 4.0 License.

this hypothesis seriously. In the end of 1933, Fermi published his most important theoretical work, an effective theory of the beta decay,⁵ which is actually a low-energy version of today's standard picture of weak charged-current interactions. Fermi's seminal work made it possible to calculate the reaction rates of nucleons and electrons (or positrons) interacting with neutrinos (or antineutrinos).

In 1936, Hans Bethe pointed out that an inverse beta decay mode of the type $\bar{\nu}_e + p \rightarrow n + e^+$ (or more general, $\bar{\nu}_e + (A, Z) \rightarrow (A, Z - 1) + e^+$) could be a possible way to verify the existence of electron antineutrinos produced from either fission bombs or fission reactors.⁶ This preliminary idea was elaborated by Bruno Pontecorvo in 1946,⁷ and it became feasible with the development of the liquid scintillation counting techniques in the 1950s. Although the incident $\bar{\nu}_e$ is invisible, it can trigger the inverse beta decay where the emitted positron annihilates with an electron and the daughter nucleus is captured in the detector. Both events are observable because they emit gamma rays, and the corresponding flashes in the liquid scintillator are separated by some microseconds. Frederick Reines and Clyde Cowan did the first reactor antineutrino experiment and obtained a positive result in 1956,⁸ and they reported a new result consistent with the parity-violating theory of weak interactions in 1960. The Nobel Prize finally came to Reines in 1995, when Cowan had passed away 21 years before.

The discovery of electron antineutrinos motivated Pontecorvo to speculate on the possibility of lepton number violation and neutrino–antineutrino transitions in 1957.⁹ His argument was actually based on a striking conjecture made by Ettore Majorana in 1937: a massive neutrino could be its own antiparticle.¹⁰

In 1962, the muon neutrino — a sister of the electron neutrino — was discovered by Leon Lederman, Melvin Schwartz and Jack Steinberger in an accelerator-based experiment.¹¹ This discovery, which immediately motivated Ziro Maki, Masami Nakagawa and Shoichi Sakata to conjecture the $\nu_e \leftrightarrow \nu_\mu$ conversion,¹² was also recognized by the Nobel Prize in 1988. The tau neutrino, another sister of the electron neutrino, was finally observed at the Fermilab in the end of 2000.¹³ Within the standard model the complete lepton family consists of three charged members (e, μ, τ) and three neutral members (ν_e, ν_μ, ν_τ), and their corresponding antiparticles.

1.2. Where do neutrinos come from?

Neutrinos and antineutrinos may originate from many physical and astrophysical processes via weak interactions. Figure 1 illustrates some typical examples of neutrino or antineutrino sources in the Universe.

Example (1): Neutrinos and antineutrinos from the Big Bang. The standard cosmology predicts the existence of a cosmic neutrino (or antineutrino) background in the Universe. Today such *relic* neutrinos and antineutrinos should have an overall number density around 330 cm^{-3} , but their temperature is so low (only about 1.9 K, or roughly $1.6 \times 10^{-4} \text{ eV}$) that there is no way to detect them. In the long run

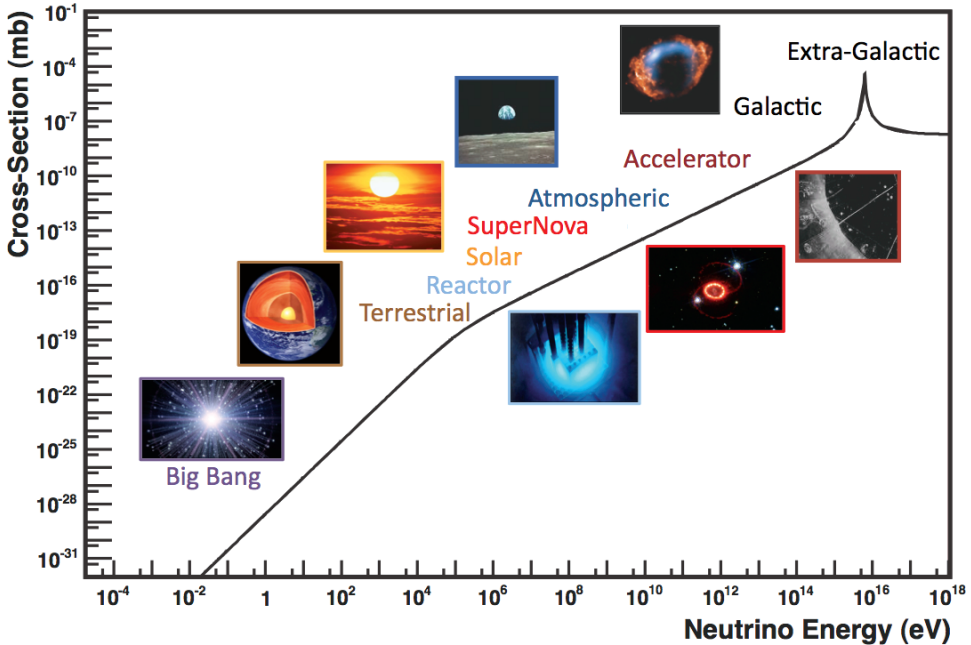


Fig. 1. Some representative sources of neutrinos and (or) antineutrinos and their corresponding energies.¹⁴ The cross sections of $\bar{\nu}_e + e^- \rightarrow \bar{\nu}_e + e^-$ scattering associated with different sources are also shown for comparison, where the peak around 6.3 PeV is related to the Glashow resonance.¹⁵

it might be possible to capture the relic electron neutrinos on some beta-decaying nuclei,¹⁶ as the PTOLEMY project is trying.¹⁷

Example (2): Electron antineutrinos from the Earth. Since its birth, the Earth's interior has kept a number of radioactive nuclei (e.g., ^{40}K , ^{238}U and ^{232}Th). That is why numerous electron antineutrinos can be produced from terrestrial “natural radioactivity” (i.e., the beta decays), at a rate of several millions per square centimeter per second. So far such interesting geo- $\bar{\nu}_e$ events have been observed at the 3σ level in the KamLAND¹⁸ and Borexino¹⁹ experiments.

Example (3): Electron neutrinos from the Sun. Solar electron neutrinos come along with a number of thermonuclear fusion reactions inside the Sun. One may understand why the Sun shines with the help of $4p \rightarrow ^4\text{He} + 2e^+ + 2\nu_e + 26.7 \text{ MeV}$: about 98% of the energy radiates in the form of light and only 2% of the energy is taken away by neutrinos.²⁰ The only way to verify such a picture on the Earth is to detect the electron neutrinos emitted from the core of the Sun. In 1968 solar neutrinos were first observed by Raymond Davis in his radiochemical experiment (see Section 4.1 for a more detailed description).²¹

Example (4): Neutrinos and antineutrinos from supernovae. The explosion of a supernova may release the gravitational binding energy of $\mathcal{O}(10^{53})$ erg in the form of neutrinos and antineutrinos.²² On 23 February 1987 the ν_e and $\bar{\nu}_e$ events from the Supernova 1987A explosion were observed by the Kamiokande-II,²³ IMB²⁴ and

Baksan²⁵ detectors. This observation was a great milestone in neutrino astronomy. Davis and Masatoshi Koshiba received the Nobel Prize in 2002 for their pioneering detections of solar and supernova neutrinos, respectively.

Example (5): Neutrinos and antineutrinos from the Earth's atmosphere. When a cosmic ray (which is mainly composed of high-energy protons coming from somewhere in the galactic or extragalactic space) penetrates the atmosphere around the Earth, it may interact with the ambient nuclei and generate a particle shower containing charged pions and muons. The decays of π^\pm and μ^\pm can therefore produce atmospheric $\nu_\mu, \bar{\nu}_\mu, \nu_e$ and $\bar{\nu}_e$ events, which have been observed in several experiments.²⁶ In particular, the phenomenon of atmospheric neutrino oscillations was firmly established by the Super-Kamiokande (SK) Collaboration in 1998.²⁷

Example (6): Ultrahigh-energy (UHE) cosmic neutrinos and antineutrinos from distant astrophysical sources, including the expected active galactic nuclei, gamma ray bursts, supernova remnants and the Greisen–Zatsepin–Kuzmin cut-off of cosmic rays.²⁹ The UHE $\nu_\mu, \bar{\nu}_\mu, \nu_e$ and $\bar{\nu}_e$ events can be produced from UHE $p\gamma$ or pp collisions via π^\pm and μ^\pm decays, and thus they may serve as a unique cosmic messenger and provide us with useful information about the cosmos that cannot be extracted from the measurements of cosmic rays and gamma rays. So far the IceCube detector at the South Pole has observed 37 extraterrestrial neutrino candidate events with deposited energies ranging from 30 TeV to 2 PeV.²⁸ Among them, the three PeV events represent the highest-energy neutrino interactions ever observed, but their astrophysical origin remains mysterious.

Of course, neutrinos and (or) antineutrinos can also be produced from some man-made facilities, especially the nuclear reactors and particle accelerators. They also play a crucial role in discovering neutrinos, observing flavor oscillations and measuring fundamental parameters, as one will see in sections 3–5.

2. Weak Interactions of Neutrinos in the Standard Theory

As an important part of the matter content in the standard electroweak model based on the $SU(2)_L \times U(1)_Y$ gauge group, neutrinos are assumed to be the *massless* Weyl particles. Hence only the left-handed neutrinos and right-handed antineutrinos exist, and they take part in weak charged- and neutral-current interactions via

$$\begin{aligned}
 -\mathcal{L}_{\text{cc}} &= \frac{g}{2\sqrt{2}} \sum_{\alpha} [\bar{\alpha} \gamma^{\mu} (1 - \gamma_5) \nu_{\alpha} W_{\mu}^{-} + \text{h.c.}], \\
 -\mathcal{L}_{\text{nc}} &= \frac{g}{4 \cos \theta_w} \sum_{\alpha} [\bar{\nu}_{\alpha} \gamma^{\mu} (1 - \gamma_5) \nu_{\alpha}] Z_{\mu},
 \end{aligned} \tag{1}$$

where $\alpha = e, \mu, \tau$. Eq. (1) allows one to calculate the cross sections of neutrino–electron, neutrino–neutrino and neutrino–nucleon scattering processes.²⁹ Note that the reactions $\nu_e + e^{-} \rightarrow \nu_e + e^{-}$ and $\bar{\nu}_e + e^{-} \rightarrow \bar{\nu}_e + e^{-}$ can happen via both charged- and neutral-current interactions, but $\nu_{\mu} + e^{-} \rightarrow \nu_{\mu} + e^{-}$ (or $\nu_{\tau} + e^{-} \rightarrow \nu_{\tau} + e^{-}$) and $\bar{\nu}_{\mu} + e^{-} \rightarrow \bar{\nu}_{\mu} + e^{-}$ (or $\bar{\nu}_{\tau} + e^{-} \rightarrow \bar{\nu}_{\tau} + e^{-}$) can only occur via the neutral-current interactions. That is why the behavior of neutrino flavor conversion in a dense

medium may be modified by the coherent forward $\nu_e e^-$ or $\bar{\nu}_e e^-$ scattering. This effect is referred to as the Wolfenstein–Mikheyev–Smirnov (MSW) matter effect.³⁰

The simplest quasi-elastic neutrino–nucleon scattering processes are the inverse beta decays $\bar{\nu}_e + p \rightarrow e^+ + n$ and $\nu_e + n \rightarrow e^- + p$, which take place via the charged-current weak interactions. Their cross sections can be approximately expressed as $\sigma(\bar{\nu}_e p) = \sigma(\nu_e n) \simeq 9.1 \times 10^{-44} (E_\nu/\text{MeV})^2 \text{cm}^2$. In comparison, the elastic neutrino–nucleon scattering reaction $\nu_\alpha + N \rightarrow \nu_\alpha + N$ (for $\alpha = e, \mu, \tau$) is mediated by the neutral-current weak interactions.

Historically, the existence of weak neutral currents was first established in the Gargamelle bubble chamber at CERN in 1973.³¹ This experiment, which observed the highly expected events of $\nu_\mu + N \rightarrow \nu_\mu + \text{hadrons}$ and $\bar{\nu}_\mu + N \rightarrow \bar{\nu}_\mu + \text{hadrons}$, crowned the long-range neutrino program initiated by CERN at that time and brought CERN a leading role in the field of high energy physics. It also provided an unprecedentedly strong support to the standard electroweak model formulated by Sheldon Glashow, Steven Weinberg and Abdus Salam in the 1960s.³² These three theorists received the Nobel Prize in 1979 for their contributions to the electroweak theory and especially for their prediction of the weak neutral current. Four years later, the three mediators of the weak force (i.e., the W^\pm and Z^0 bosons) were finally discovered by Carlo Rubbia and his colleagues at CERN.³³

The standard theory was thoroughly tested in the 1990s with the help of the Large Electron–Positron Collider (LEP) running on the Z^0 resonance at CERN. In particular, the number of neutrino species was determined to be $N_\nu = 2.984 \pm 0.008$ via the decay $Z^0 \rightarrow \nu_\alpha + \bar{\nu}_\alpha$.²⁶ Such a result is consistent very well with 3 as required in the theory. Extra light neutrino species are not impossible, but they must be “sterile” — in the sense that they do not directly take part in the standard weak interactions, and hence their existence is not subject to the LEP measurement.

Note that the structure of the standard theory itself is too economical to allow the neutrinos to be massive. On the one hand, the particle content of the model is so limited that there are neither right-handed neutrinos nor any Higgs triplets. Hence a normal Dirac neutrino mass term is not allowed, nor a gauge-invariant Majorana mass term. On the other hand, the model is a renormalizable quantum field theory. The renormalizability implies that an effective dimension-5 operator, which can give each neutrino a Majorana mass, is also forbidden.

3. Neutrino Masses, Flavor Mixing and Oscillations

3.1. Massive neutrinos and their electromagnetic properties

There are several ways to slightly extend the standard theory such that the neutrinos can acquire their masses with little influence on the great success of the theory itself.³⁴ Here let us take two typical examples for illustration.

(1) If the renormalizability of the standard theory is relaxed, then the lowest-dimension operator that violates lepton number and generates neutrino masses must be the unique dimension-5 Weinberg operator $HH\ell\ell/\Lambda$, where Λ denotes the cut-off

energy scale in such an effective field theory, H and ℓ are the Higgs and lepton doublets, respectively.³⁵ After spontaneous gauge symmetry breaking, this operator yields the neutrino masses $m_i \sim \langle H \rangle^2 / \Lambda$ (for $i = 1, 2, 3$), which can be sufficiently small ($\lesssim 1$ eV) provided $\Lambda \gtrsim 10^{13}$ GeV and $\langle H \rangle \sim 10^2$ GeV. In this sense the study of neutrino mass generation can serve as a striking low-energy window onto new physics at superhigh energy scales.

(2) If two or more heavy right-handed neutrinos are added into the standard theory and lepton number is violated by their Majorana mass term, then the Lagrangian responsible for neutrino masses can be written as

$$-\mathcal{L}_{\text{mass}} = \overline{\ell}_L Y_\nu \tilde{H} N_R + \frac{1}{2} \overline{N}_R^c M_R N_R + \text{h.c.}, \quad (2)$$

in which the first term stands for the neutrino Yukawa interactions, and the second term is lepton-number-violating. After the $SU(2)_L \times U(1)_Y$ gauge symmetry is spontaneously broken to $U(1)_{\text{em}}$, one is left with the effective Majorana neutrino mass matrix $M_\nu \simeq -\langle H \rangle^2 Y_\nu M_R^{-1} Y_\nu^T$, which is often referred to as the canonical *seesaw* formula.³⁶ Because N_R is the $SU(2)_L$ singlet, the mass scale of M_R can be greatly higher than the electroweak scale $\langle H \rangle$. Hence the mass scale of M_ν is highly suppressed, providing a natural explanation of the smallness of neutrino masses.

Instead of introducing the heavy right-handed neutrinos, one may also introduce a Higgs triplet or a few triplet fermions into the standard theory so as to explain why the three active neutrinos should have naturally small masses.²⁹ Such seesaw mechanisms essentially have the same spirit, which attributes the smallness of neutrino masses to the largeness of new degrees of freedom. Furthermore, they require massive neutrinos to be the Majorana particles and thus allow some lepton-number-violating processes to happen.

It is worth pointing out that a pure Dirac neutrino mass term, originating from the neutrino Yukawa interactions on the right-hand side of Eq. (2), is less convincing and less interesting from a theoretical point of view. The reason for this argument is two-fold: (a) such a scenario cannot explain why the neutrino masses are so small as compared with the charged lepton masses; (b) given N_R , the lepton-number-violating term $\overline{N}_R^c M_R N_R$ should not be absent because it is not forbidden by gauge symmetry and Lorentz invariance. If massive neutrinos really have the Majorana nature, they can trigger the neutrinoless double-beta ($0\nu\beta\beta$) decays and some other lepton-number-violating processes. In particular, they are likely to have something to do with the observed asymmetry of matter and antimatter in the Universe via the seesaw and leptogenesis³⁷ mechanisms. Hence the phenomenology of Majorana neutrinos is much richer and more interesting than that of Dirac neutrinos.

Although a massive neutrino does not possess any electric charge, it can have electromagnetic interactions via quantum loops.³⁸ Now that Dirac and Majorana neutrinos couple to the photon in different ways, their corresponding electromagnetic form factors must be different. Given the standard weak interactions, one finds that a massive Dirac neutrino has no electric dipole moment and its magnetic dipole

moment is finite but extremely small: $\mu_\nu \sim 3 \times 10^{-20} (m_\nu/0.1 \text{ eV}) \mu_B$ with μ_B being the Bohr magneton. In contrast, a massive Majorana neutrino has neither electric nor magnetic dipole moments, simply because its antiparticle is just itself.

But both Dirac and Majorana neutrinos can have the *transition* dipole moments (i.e., from one mass eigenstate to another mass eigenstate), which may result in neutrino decays, neutrino–electron scattering, neutrino interactions with external magnetic fields, etc.³⁹ In a realistic neutrino–electron scattering experiment, what can be constrained is actually an effective transition dipole moment μ_{eff} consisting of both electric and magnetic components. Hence it is practically impossible to distinguish between Dirac and Majorana neutrinos in such measurements. Current experimental upper bounds on μ_{eff} are at the level of $10^{-11} \mu_B$,³⁹ far above the afore-mentioned theoretical expectation $\mu_\nu \sim 10^{-20} \mu_B$.

3.2. Lepton flavor mixing and neutrino oscillations

In the basis where the flavor eigenstates of three charged leptons are identified with their mass eigenstates, one may diagonalize the Majorana neutrino mass matrix M_ν by means of a unitary transformation. Then the leptonic charged-current interactions in Eq. (1) can be reexpressed in terms of the mass eigenstates:

$$-\mathcal{L}_{\text{cc}} = \frac{g}{\sqrt{2}} \overline{(e \ \mu \ \tau)}_L \gamma^\mu U \begin{pmatrix} \nu_1 \\ \nu_2 \\ \nu_3 \end{pmatrix}_L W_\mu^- + \text{h.c.}, \quad (3)$$

where the 3×3 unitary matrix U describes the strength of lepton flavor mixing and can be parameterized by using three rotation angles and three CP-violating phases:

$$U = \begin{pmatrix} c_{12}c_{13} & s_{12}c_{13} & s_{13}e^{-i\delta} \\ -s_{12}c_{23} - c_{12}s_{13}s_{23}e^{i\delta} & c_{12}c_{23} - s_{12}s_{13}s_{23}e^{i\delta} & c_{13}s_{23} \\ s_{12}s_{23} - c_{12}s_{13}c_{23}e^{i\delta} & -c_{12}s_{23} - s_{12}s_{13}c_{23}e^{i\delta} & c_{13}c_{23} \end{pmatrix} P_\nu, \quad (4)$$

where $c_{ij} \equiv \cos \theta_{ij}$, $s_{ij} \equiv \sin \theta_{ij}$ (for $ij = 12, 13, 23$), δ is referred to as the Dirac CP-violating phase, and $P_\nu = \text{Diag} \{e^{i\rho}, e^{i\sigma}, 1\}$ contains two extra phase parameters of the Majorana nature. The matrix U is often called the Pontecorvo–Maki–Nakagawa–Sakata (PMNS) matrix, and its unitarity has been tested at the percent level.^{40, a}

Equation (3) tells us that a ν_α neutrino can be produced from the $W^+ + \alpha^- \rightarrow \nu_\alpha$ interaction, and a ν_β neutrino can be detected through the $\nu_\beta + W^- \rightarrow \beta^-$ interaction (for $\alpha, \beta = e, \mu, \tau$). The $\nu_\alpha \rightarrow \nu_\beta$ oscillation may happen if the ν_i beam

^aNote that whether U is unitary or not depends on the mechanism of neutrino mass generation. In the canonical seesaw mechanism,³⁶ for instance, the mixing between light and heavy Majorana neutrinos may lead to tiny unitarity-violating effects for the PMNS matrix U itself.

with energy $E \gg m_i$ travels a proper distance L in vacuum. The probability of such a flavor oscillation is given by²⁹

$$P(\nu_\alpha \rightarrow \nu_\beta) = \delta_{\alpha\beta} - 4 \sum_{i < j} \left(\text{Re} \diamond_{\alpha\beta}^{ij} \sin^2 \Delta_{ji} \right) + 8 \text{Im} \diamond_{\alpha\beta}^{ij} \prod_{i < j} \sin \Delta_{ji}, \quad (5)$$

in which $\Delta_{ji} \equiv \Delta m_{ji}^2 L / (4E)$ and $\diamond_{\alpha\beta}^{ij} \equiv U_{\alpha i} U_{\beta j} U_{\alpha j}^* U_{\beta i}^*$ (for $i, j = 1, 2, 3$ and $\alpha, \beta = e, \mu, \tau$). The probability of the $\bar{\nu}_\alpha \rightarrow \bar{\nu}_\beta$ oscillation can easily be read off from Eq. (5) by making the replacement $U \rightarrow U^*$. There are two types of neutrino oscillation experiments: the ‘‘appearance’’ one ($\alpha \neq \beta$) and the ‘‘disappearance’’ one ($\alpha = \beta$). Both solar neutrino oscillations ($\nu_e \rightarrow \nu_e$) and reactor antineutrino oscillations ($\bar{\nu}_e \rightarrow \bar{\nu}_e$) are of the disappearance type. The atmospheric muon-neutrino (or muon-antineutrino) oscillations essentially belong to the disappearance type, and the accelerator neutrino oscillations can be of either type.

At this point let us explain why it is extremely difficult to do a realistic neutrino-antineutrino oscillation experiment. We consider an $\bar{\nu}_\alpha$ beam produced from the standard charged-current interactions $\alpha^+ + W^- \rightarrow \bar{\nu}_\alpha$. After traveling a distance L this beam will be detected at a detector through the standard charged-current interactions $\nu_\beta \rightarrow \beta^- + W^+$. Different from the normal $\nu_\alpha \rightarrow \nu_\beta$ or $\bar{\nu}_\alpha \rightarrow \bar{\nu}_\beta$ oscillations, the $\bar{\nu}_\alpha \rightarrow \nu_\beta$ oscillation involves a suppression factor m_i/E in its amplitude. This factor reflects the fact that the incoming α^+ leads to an antineutrino $\bar{\nu}_\alpha$ in a dominantly right-handed helicity state, whereas the standard charged-current interactions that produce the outgoing β^- would prefer the incident neutrino ν_β being in a left-handed state.⁴¹ Because of $m_i \lesssim 1$ eV and $E \gtrsim 1$ MeV in a realistic experiment, this helicity suppression factor (i.e., $m_i/E \lesssim 10^{-6}$) makes it impossible to observe the phenomenon of neutrino-antineutrino oscillations.

4. Observations of Neutrino Oscillations

4.1. Solar neutrino oscillations

In 1946 Pontecorvo put forward a radiochemical technique which can be used to measure solar electron neutrinos via the reaction $^{37}\text{Cl} + \nu_e \rightarrow ^{37}\text{Ar} + e^-$.⁷ The incident neutrino’s energy threshold for this reaction to happen is 0.814 MeV, low enough to make it sensitive to solar ^8B neutrinos. In 1964 John Bahcall carefully calculated the solar neutrino flux and the capture rate of ^8B neutrinos, demonstrating the experimental feasibility of Pontecorvo’s idea.⁴² This motivated Davis to build a 10⁵-gallon Chlorine-Argon neutrino detector in the Homestake Gold Mine in the middle of the 1960s. The final result of this experiment was published in 1968 and caused a big puzzle: the measured flux of solar ^8B neutrinos was only about one third of the value predicted by the standard solar model (SSM).²¹ Such a deficit was later confirmed in a number of solar neutrino experiments, including the Homestake,⁴³ GALLEX/GNO,⁴⁴ SAGE,⁴⁵ SK⁴⁶ and SNO⁴⁷ experiments. Among them, the SNO experiment was especially crucial because it model-independently

demonstrated the flavor conversion of solar ν_e neutrinos into ν_μ and ν_τ neutrinos.

Given heavy water as the target material of the SNO detector, the solar ^8B neutrinos were measured via the charged-current (CC) reaction $\nu_e + \text{D} \rightarrow e^- + \text{p} + \text{p}$, the neutral-current (NC) reaction $\nu_\alpha + \text{D} \rightarrow \nu_\alpha + \text{p} + \text{n}$ and the elastic-scattering process $\nu_\alpha + e^- \rightarrow \nu_\alpha + e^-$ (for $\alpha = e, \mu, \tau$).⁴⁷ The observed neutrino fluxes in these three different channels are expected to satisfy $\phi_{\text{CC}} = \phi_e$, $\phi_{\text{NC}} = \phi_e + \phi_{\mu\tau}$ and $\phi_{\text{ES}} = \phi_e + 0.155\phi_{\mu\tau}$, where $\phi_{\mu\tau}$ denotes a sum of the fluxes of ν_μ and ν_τ neutrinos. So $\phi_{\text{CC}} = \phi_{\text{NC}} = \phi_{\text{ES}}$ would hold if there were no flavor conversion (i.e., $\phi_{\mu\tau} = 0$). The SNO data $\phi_{\text{CC}} = 1.68^{+0.06}_{-0.06}(\text{stat})_{-0.09}(\text{syst})$, $\phi_{\text{NC}} = 4.94^{+0.21}_{-0.21}(\text{stat})_{-0.34}(\text{syst})$ and $\phi_{\text{ES}} = 2.35^{+0.22}_{-0.22}(\text{stat})_{-0.15}(\text{syst})$ as illustrated in Fig. 2 from Ref. 48 definitely demonstrated $\phi_{\mu\tau} \neq 0$. Now we are sure that the deficit of solar ^8B neutrinos, whose typical energies are about 6 MeV to 7 MeV, is due to $\nu_e \rightarrow \nu_\mu$ and $\nu_e \rightarrow \nu_\tau$ oscillations modified by significant MSW matter effects in the Sun. A careful analysis shows that the observed survival probability of solar ^8B neutrino oscillations can approximate to $P(\nu_e \rightarrow \nu_e) \simeq \sin^2 \theta_{12} \simeq 0.32$,⁴⁹ leading us to $\theta_{12} \simeq 34^\circ$.

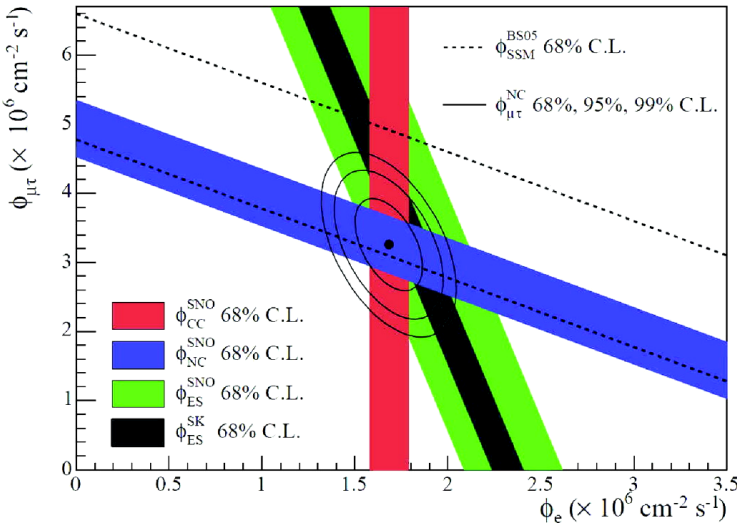


Fig. 2. The $\nu_\mu + \nu_\tau$ flux versus the ν_e flux determined from the SNO data. The total solar ^8B neutrino flux predicted by the SSM is shown as dashed lines, parallel to the NC measurement. The narrowed band parallel to the SNO's ES measurement corresponds to the SK's ES result. The best-fit point is obtained by using only the SNO data.⁴⁸

Moreover, the Borexino experiment has accomplished a real-time measurement of the mono-energetic solar ^7Be neutrinos with $E = 0.862$ MeV and observed a remarkable deficit corresponding to $P(\nu_e \rightarrow \nu_e) = 0.56 \pm 0.1$.⁵⁰ Such a result can roughly be explained as a vacuum oscillation effect, because the low-energy ^7Be neutrino oscillation is not very sensitive to matter effects.⁴⁹ In this case we are left

with the averaged survival probability $P(\nu_e \rightarrow \nu_e) \simeq 1 - \sin^2 2\theta_{12}/2 \simeq 0.56$ as a reasonable approximation for solar ${}^7\text{Be}$ neutrinos, and thus obtain $\theta_{12} \simeq 35^\circ$. This result is essentially consistent with the one extracted from solar ${}^8\text{B}$ neutrinos.

4.2. Atmospheric neutrino oscillations

The atmospheric ν_μ , $\bar{\nu}_\mu$, ν_e and $\bar{\nu}_e$ events are produced in the Earth's atmosphere by cosmic rays, mainly via the decays $\pi^+ \rightarrow \mu^+ + \nu_\mu$ with $\mu^+ \rightarrow e^+ + \nu_e + \bar{\nu}_\mu$ and $\pi^- \rightarrow \mu^- + \bar{\nu}_\mu$ with $\mu^- \rightarrow e^- + \bar{\nu}_e + \nu_\mu$. So the ratio of ν_μ and $\bar{\nu}_\mu$ events to ν_e and $\bar{\nu}_e$ events is expected to be nearly 2 : 1 at low energies ($\lesssim 1$ GeV). But a smaller ratio was observed at the Kamiokande⁵¹ and IMB⁵² detectors in the late 1980s and early 1990s, indicating a preliminary deficit of atmospheric muon neutrinos and muon antineutrinos. If there were no neutrino oscillation, the atmospheric neutrinos that enter and excite an underground detector would have an almost perfect spherical symmetry. Namely, the downward-going and upward-going neutrino fluxes should be equal to each other, or equivalently $\Phi_e(\theta_z) = \Phi_e(\pi - \theta_z)$ and $\Phi_\mu(\theta_z) = \Phi_\mu(\pi - \theta_z)$ for the zenith angle θ_z . In 1998 the SK Collaboration observed an approximate up-down flux symmetry for atmospheric ν_e and $\bar{\nu}_e$ events and a significant up-down flux asymmetry for atmospheric ν_μ and $\bar{\nu}_\mu$ events.²⁷

The SK detector is a 5×10^4 -ton tank of ultra-pure water, located approximately 1 km underground in the Mozumi Mine in Kamioka. As illustrated in Fig. 3, the inside surface of the tank is lined with more than 1.1×10^4 photo-multiplier tubes (PMTs). An additional layer of water called the outer detector is also instrumented PMTs to detect any charged particles entering the central volume and to shield the inner detector by absorbing any neutrons produced in the nearby rock. A neutrino

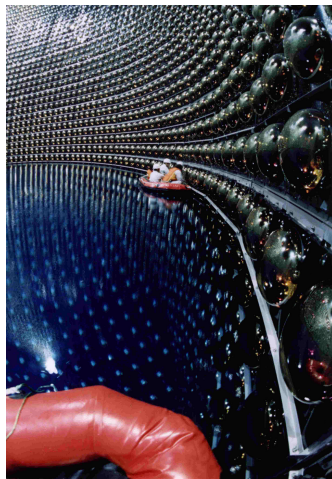


Fig. 3. A brief view from inside the SK detector's water tank during filling.²⁷ SK image copyright: Kamioka Observatory, ICRR (Institute for Cosmic Ray Research), The University of Tokyo.

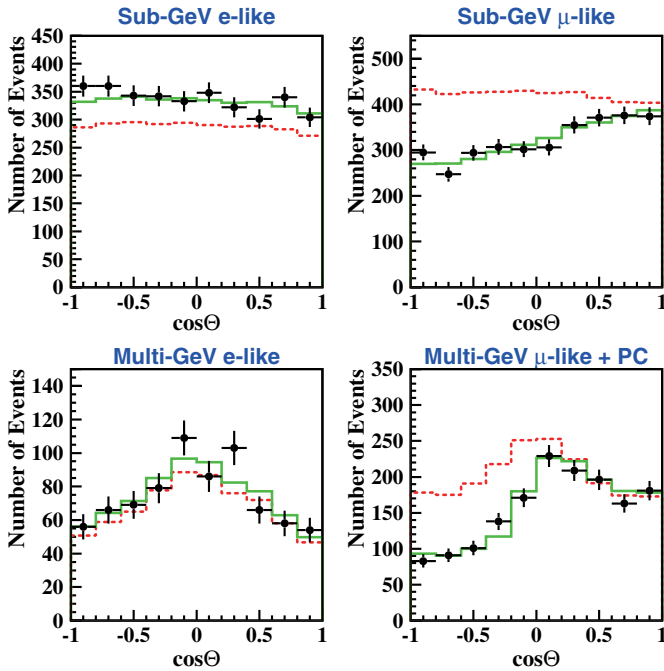


Fig. 4. The SK zenith-angle distributions for fully contained 1-ring e -like and μ -like events with visible energy <1.33 GeV (sub-GeV) and >1.33 GeV (multi-GeV). For multi-GeV μ -like events, a combined distribution with partially contained events is illustrated. The dotted histograms show the non-oscillation Monte Carlo events, and the solid histograms show the best-fit expectations for atmospheric $\nu_\mu \rightarrow \nu_\mu$ oscillations.²⁶

interacting with the electrons or nuclei of water can produce a charged particle that moves faster than the speed of light in water, creating a cone of light known as Cherenkov radiation. The Cherenkov light is projected as a ring on the wall of the detector and recorded by the PMTs. Hence the direction and flavor of an incident neutrino can be identified by using the details of the ring pattern.

As shown in Fig. 4, the observed deficit of atmospheric upward-going ν_μ and $\bar{\nu}_\mu$ events at SK could naturally be attributed to $\nu_\mu \rightarrow \nu_\tau$ and $\bar{\nu}_\mu \rightarrow \bar{\nu}_\tau$ oscillations, because the detector itself was insensitive to ν_τ and $\bar{\nu}_\tau$ events. This was actually the first *model-independent* evidence for neutrino oscillations, and it marked the threshold of a new era in particle physics. Since 1998 a number of breakthroughs have been made in experimental neutrino physics.

In 2004 the SK Collaboration carried out a careful analysis of the ν_μ (or $\bar{\nu}_\mu$) disappearance probability as a function of the neutrino flight length L over the neutrino energy E , and observed a dip in the L/E distribution as the first *direct* evidence for atmospheric neutrino oscillations.⁵³ This dip was consistent with the prediction from the sinusoidal flavor transition probability of neutrino oscillations, but inconsistent with the exotic neutrino decay and neutrino decoherence scenarios.

To directly observe the atmospheric $\nu_\mu \rightarrow \nu_\tau$ oscillation is quite difficult because it requires the neutrino beam energy greater than a threshold of 3.5 GeV, such that a tau lepton can be produced via the charged-current interaction of incident ν_τ with the target nuclei in the detector. But the SK data are found to be best described by neutrino oscillations that include the ν_τ appearance in addition to the overwhelming signature of the ν_μ disappearance. A neural network analysis of the zenith-angle distribution of multi-GeV contained events has recently demonstrated this observation at the 3.8σ level.⁵⁴

4.3. Accelerator neutrino oscillations

If the observed deficit of atmospheric ν_μ and $\bar{\nu}_\mu$ events is ascribed to neutrino oscillations, then a fraction of the accelerator-produced ν_μ and $\bar{\nu}_\mu$ events should also disappear on their way to a remote detector. This expectation has definitely been confirmed by two long-baseline neutrino oscillation experiments: K2K⁵⁵ and MINOS.⁵⁶ The K2K experiment was designed in such a way that the ν_μ beam was produced at the KEK accelerator and measured 250 km away at the SK detector in Kamioka. In comparison, the baseline length of the MINOS experiment is 735 km, from the source of ν_μ neutrinos at Fermilab to the far detector in northern Minnesota. Both of them have observed a reduction of the ν_μ flux and a distortion of the ν_μ energy spectrum, implying $\nu_\mu \rightarrow \nu_\mu$ oscillations. The most striking result obtained from the atmospheric and accelerator neutrino oscillation experiments is $\sin^2 2\theta_{23} \simeq 1$ or $\theta_{23} \simeq 45^\circ$, which might hint at a special flavor structure or a certain flavor symmetry in the neutrino sector.⁵⁷

An especially important accelerator neutrino oscillation experiment is the T2K experiment with a ν_μ beam produced from the J-PARC Main Ring in Tokai and pointing to the SK detector at a distance of 295 km. Its main goal is to discover $\nu_\mu \rightarrow \nu_e$ appearance oscillations and perform a precision measurement of $\nu_\mu \rightarrow \nu_\mu$ disappearance oscillations. Since its preliminary data were first released in June 2011, the T2K experiment has proved to be very successful in establishing the ν_e appearance out of a ν_μ beam at the 7.3σ level and constraining the neutrino mixing parameters θ_{13} , θ_{23} and δ .⁵⁸ The point is that the leading term of $P(\nu_\mu \rightarrow \nu_e)$ is sensitive to $\sin^2 2\theta_{13} \sin^2 \theta_{23}$, and its sub-leading term is sensitive to δ and terrestrial matter effects.⁵⁹ Figure 5 shows the allowed region of $\sin^2 2\theta_{13}$ changing with the CP-violating phase δ as constrained by the T2K data,⁵⁸ from which one can see an unsuppressed value of θ_{13} together with a preliminary hint $\delta \sim -\pi/2$ even though the neutrino mass ordering (i.e., the sign of Δm_{32}^2) remains undetermined.

Different from the K2K, MINOS and T2K experiments, the OPERA experiment was designed to search for the ν_τ appearance in a ν_μ beam traveling from CERN to Gran Sasso at a distance of 730 km. After several years of data taking, the OPERA Collaboration reported four ν_τ candidate events in 2014. These events are consistent with $\nu_\mu \rightarrow \nu_\tau$ oscillations with the 4.2σ significance.⁶⁰

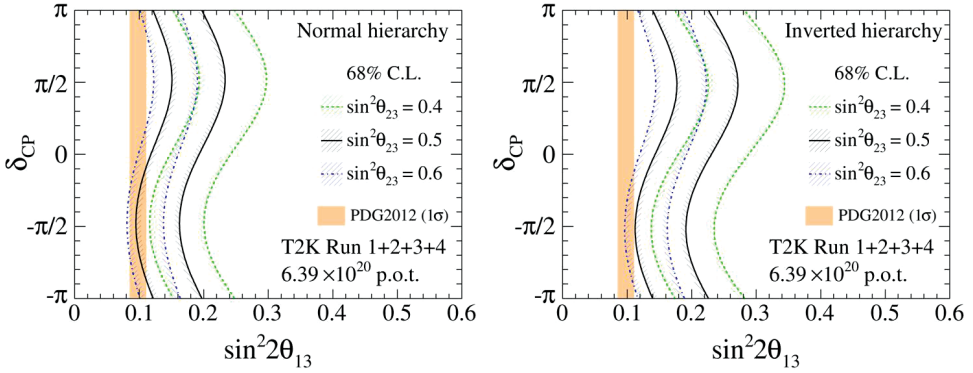


Fig. 5. The allowed region of $\sin^2 2\theta_{13}$ as a function of the CP-violating phase δ , constrained by the present T2K neutrino oscillation data.⁵⁸

4.4. Reactor antineutrino oscillations

Since the first discovery of electron antineutrinos with the help of the Savannah River reactor in 1956,⁸ reactors have been playing an important role in neutrino physics. In particular, two of the three neutrino mixing angles (θ_{12} and θ_{13}) have been measured in the KamLAND⁶¹ and Daya Bay⁶² reactor antineutrino oscillation experiments to an unprecedentedly good degree of accuracy.

The average baseline length of the KamLAND experiment was $L = 180$ km, and hence it was sensitive to the Δm_{21}^2 -driven $\bar{\nu}_e \rightarrow \bar{\nu}_e$ oscillation and allowed a terrestrial test of the large-mixing-angle (LMA) MSW solution to the solar neutrino problem. Under CPT invariance the KamLAND measurement⁶¹ firmly established the LMA solution for the first time, and pinned down the correct parameter space of solar $\nu_e \rightarrow \nu_e$ oscillations constrained by the SNO and SK experiments, as shown in Fig. 6 in the two-flavor scheme.⁶³ A striking sinusoidal behavior of $P(\bar{\nu}_e \rightarrow \bar{\nu}_e)$ against L/E was also demonstrated in the KamLAND experiment.⁶³

While the CHOOZ⁶⁴ and Palo Verde⁶⁵ reactor antineutrino experiments tried to search for the Δm_{31}^2 -driven $\bar{\nu}_e \rightarrow \bar{\nu}_e$ oscillations at the end of the 20th century, they found no indication in favor of such oscillations and thus set an upper bound on the smallest neutrino mixing angle θ_{13} . This situation has been changed by the Daya Bay,⁶² RENO⁶⁶ and Double Chooz⁶⁷ experiments in the past few years.

The Daya Bay experiment was designed to probe the smallest neutrino mixing angle θ_{13} with an unprecedented sensitivity $\sin^2 2\theta_{13} \sim 1\%$ by measuring the Δm_{31}^2 -driven $\bar{\nu}_e \rightarrow \bar{\nu}_e$ oscillation with a baseline length $L \simeq 2$ km. In this experiment the electron antineutrino beam takes its source at the Daya Bay nuclear power complex located in Shenzhen, as shown in Fig. 7. The eight antineutrino detectors deployed at the near (two plus two) and far (four) sites are all the liquid scintillator detectors.

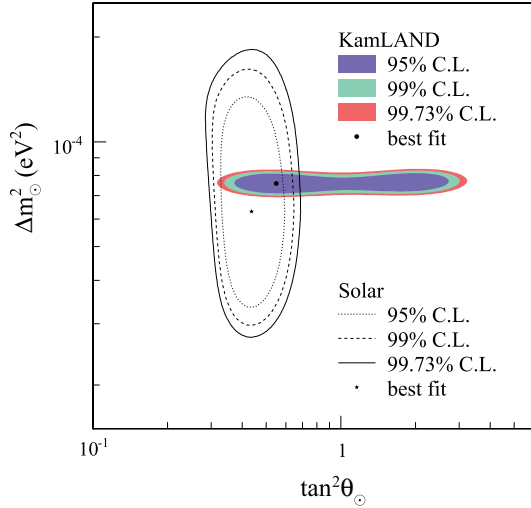


Fig. 6. The allowed region for two-flavor neutrino oscillation parameters from the KamLAND and solar neutrino experiments, where $\Delta m_{\odot}^2 \simeq \Delta m_{21}^2$ and $\tan^2 \theta_{\odot} \simeq \tan^2 \theta_{12}$ hold.⁶³

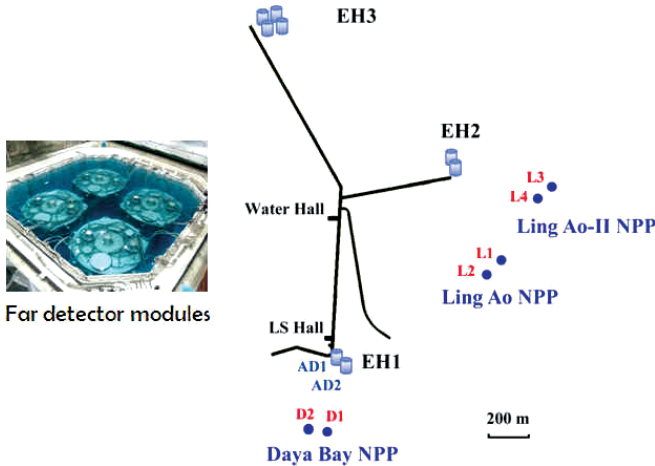


Fig. 7. The layout of the Daya Bay reactor antineutrino experiment with three pairs of reactor cores (Daya Bay, Ling Ao I and Ling Ao II). Four detector modules are deployed at the far site, and two detector modules are deployed at each of the two near sites.⁶²

In March 2012 the Daya Bay Collaboration announced a 5.2σ discovery of $\theta_{13} \neq 0$, with $\sin^2 2\theta_{13} = 0.092 \pm 0.016(\text{stat}) \pm 0.005(\text{syst})$ (see Fig. 8 for illustration).⁶² A similar but slightly less significant result was later achieved in the RENO⁶⁶ and Double Chooz⁶⁷ reactor antineutrino experiments.

The Daya Bay Collaboration has also measured the energy dependence of $\bar{\nu}_e$ disappearance and observed a nearly full oscillation cycle against L/E .⁶⁸ An improved result of the oscillation amplitude $\sin^2 2\theta_{13} = 0.090_{-0.009}^{+0.008}$ has recently been obtained

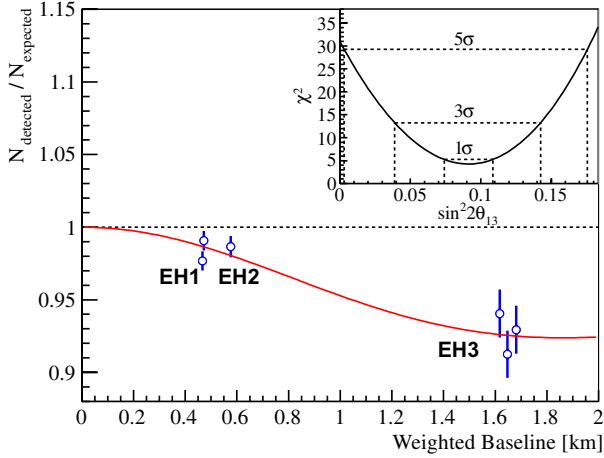


Fig. 8. The survival probability of $\bar{\nu}_e \rightarrow \bar{\nu}_e$ oscillations observed at the near and far experimental halls (i.e., EH1, EH2 and EH3) in the Daya Bay experiment.⁶²

by using the observed $\bar{\nu}_e$ rate and the observed energy spectrum in the three-flavor framework.⁶⁸ The relative large value of θ_{13} is very encouraging for the next-generation precision neutrino experiments, which aim to determine the neutrino mass ordering and probe leptonic CP violation in the foreseeable future.

4.5. Determination of oscillation parameters

The aforementioned neutrino or antineutrino oscillation experiments involve different sources, different flavors, different energies and different baseline lengths. But the relevant experimental data can all be explained in the scheme of three-flavor oscillations, which depend on two independent neutrino mass-squared differences ($\Delta m_{21}^2, \Delta m_{32}^2$), three flavor mixing angles ($\theta_{12}, \theta_{13}, \theta_{23}$) and one CP-violating phase (δ). A global fit of all the available experimental data is therefore needed in order to determine or constrain the six oscillation parameters.

A global three-flavor analysis of current experimental data on solar (SNO, SK, Borexino), atmospheric (SK), accelerator (MINOS, T2K) and reactor (KamLAND, Daya Bay, RENO) neutrino or antineutrino oscillations has recently been done by several groups.^{69–71} For the sake of simplicity, here we only quote the main results obtained by the Italian group,^{69,b} as listed in Table 1.

Table 1 shows that the output values of θ_{13}, θ_{23} and δ in such a global fit are sensitive to the sign of Δm_{31}^2 . That is why it is crucial to determine the neutrino mass ordering in the upcoming neutrino oscillation experiments. The hint $\delta \neq 0^\circ$ (or 180°) at the 1σ level is still preliminary but quite encouraging, because

^bIn this reference the notations $\delta m^2 \equiv m_2^2 - m_1^2$ and $\Delta m^2 \equiv m_3^2 - (m_1^2 + m_2^2)/2$ are used. Their relations with Δm_{21}^2 and Δm_{31}^2 are rather simple: $\Delta m_{21}^2 = \delta m^2$ and $\Delta m_{31}^2 = \Delta m^2 + \delta m^2/2$.

Table 1. The three-flavor neutrino oscillation parameters determined or constrained from a global analysis of current experimental data.⁶⁹

| Parameter | Best fit | 1σ range | 2σ range | 3σ range |
|---|----------|-----------------|----------------------------------|-----------------|
| Normal neutrino mass ordering ($m_1 < m_2 < m_3$) | | | | |
| $\Delta m_{21}^2/10^{-5} \text{ eV}^2$ | 7.54 | 7.32 — 7.80 | 7.15 — 8.00 | 6.99 — 8.18 |
| $\Delta m_{31}^2/10^{-3} \text{ eV}^2$ | 2.47 | 2.41 — 2.53 | 2.34 — 2.59 | 2.26 — 2.65 |
| $\sin^2 \theta_{12}/10^{-1}$ | 3.08 | 2.91 — 3.25 | 2.75 — 3.42 | 2.59 — 3.59 |
| $\sin^2 \theta_{13}/10^{-2}$ | 2.34 | 2.15 — 2.54 | 1.95 — 2.74 | 1.76 — 2.95 |
| $\sin^2 \theta_{23}/10^{-1}$ | 4.37 | 4.14 — 4.70 | 3.93 — 5.52 | 3.74 — 6.26 |
| $\delta/180^\circ$ | 1.39 | 1.12 — 1.77 | 0.00 — 0.16 \oplus 0.86 — 2.00 | 0.00 — 2.00 |
| Inverted neutrino mass ordering ($m_3 < m_1 < m_2$) | | | | |
| $\Delta m_{21}^2/10^{-5} \text{ eV}^2$ | 7.54 | 7.32 — 7.80 | 7.15 — 8.00 | 6.99 — 8.18 |
| $\Delta m_{13}^2/10^{-3} \text{ eV}^2$ | 2.42 | 2.36 — 2.48 | 2.29 — 2.54 | 2.22 — 2.60 |
| $\sin^2 \theta_{12}/10^{-1}$ | 3.08 | 2.91 — 3.25 | 2.75 — 3.42 | 2.59 — 3.59 |
| $\sin^2 \theta_{13}/10^{-2}$ | 2.40 | 2.18 — 2.59 | 1.98 — 2.79 | 1.78 — 2.98 |
| $\sin^2 \theta_{23}/10^{-1}$ | 4.55 | 4.24 — 5.94 | 4.00 — 6.20 | 3.80 — 6.41 |
| $\delta/180^\circ$ | 1.31 | 0.98 — 1.60 | 0.00 — 0.02 \oplus 0.70 — 2.00 | 0.00 — 2.00 |

it implies a potential effect of leptonic CP violation which is likely to show up in some long-baseline neutrino oscillation experiments in the foreseeable future. The possibility $\theta_{23} = 45^\circ$ cannot be ruled out at the 2σ level, and thus a more precise determination of θ_{23} is required in order to resolve its octant.

It is worth pointing out that $|U_{\mu i}| = |U_{\tau i}|$ (for $i = 1, 2, 3$), the so-called μ - τ permutation symmetry of the PMNS matrix U itself, holds if either the conditions $\theta_{13} = 0^\circ$ and $\theta_{23} = 45^\circ$ or the conditions $\delta = 90^\circ$ (or 270°) and $\theta_{23} = 45^\circ$ are satisfied.⁷² Now that $\theta_{13} = 0^\circ$ has definitely been excluded, it is imperative to know the values of θ_{23} and δ as accurately as possible, so as to fix the strength of μ - τ symmetry breaking associated with the structure of U .

5. Neutrino Mass Ordering and CP Violation

The neutrino mass ordering can be explored with either reactor electron antineutrinos or atmospheric muon neutrinos in the “disappearance” oscillation experiments, or with accelerator muon neutrinos in the “appearance” oscillation experiments. Let us take the JUNO,⁷³ PINGU⁷⁴ and LBNE⁷⁵ experiments for example to illustrate the future prospects in this regard.

The JUNO electron antineutrino detector is expected to be a 20-kiloton liquid-scintillator detector located in the Jiangmen city of Guangdong province in southern China, about 53 km away from the Yangjiang (17.4 GW_{th}) and Taishan (18.4 GW_{th}) reactor facilities which serve as the $\bar{\nu}_e$ source. Given Eq. (5), the survival probability

of $\bar{\nu}_e \rightarrow \bar{\nu}_e$ oscillations can be explicitly expressed as

$$P(\bar{\nu}_e \rightarrow \bar{\nu}_e) = 1 - \sin^2 2\theta_{12} \cos^4 \theta_{13} \sin^2 \Delta_{21} - \frac{1}{2} \sin^2 2\theta_{13} [1 - \cos \Delta_* \cos \Delta_{21} + \cos 2\theta_{12} \sin \Delta_* \sin \Delta_{21}], \quad (6)$$

where $\Delta_* \equiv \Delta_{31} + \Delta_{32}$. In Eq. (6) the oscillating argument Δ_{21} is unambiguous, and the neutrino mass ordering is determined by the sign of Δ_* (normal: positive; inverted: negative). To distinguish the inverted neutrino mass hierarchy from the normal one, it is necessary to measure the Δ_* -driven oscillations over many cycles on condition that $\Delta_{21} \sim \pi/2$ is satisfied for $L \sim 53$ km as taken in the JUNO experiment.⁷⁶ Figure 9 illustrates why this idea works.

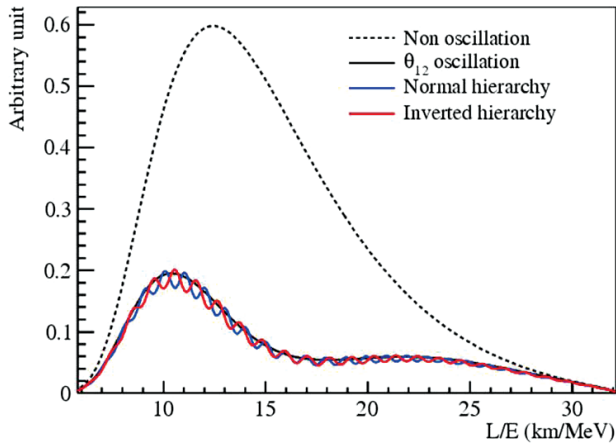


Fig. 9. The reactor antineutrino spectrum changing with L/E at a baseline $L \sim 53$ km, where the blue (normal) or red (inverted) fine structure can tell the neutrino mass hierarchy after a Fourier transformation of the spectrum.⁷⁶

Now the JUNO experiment's civil construction is underway, and its detector assembly is planned for 2018 to 2019. Data taking will commence in 2020, with a target of about six years of operation to pin down the neutrino mass ordering at the 3σ or 4σ level.⁷³ The challenges for this experiment, which must be met successfully, are mainly technological, such as how to improve the scintillator light yield, attenuation length and PMT quantum efficiency.⁷⁷

The PINGU experiment is a proposed low-energy infill extension of the IceCube experiment at the South Pole.⁷⁴ Its design closely follows the one used for IceCube and DeepCore. The idea is to further infill the central DeepCore volume with 40 new strings of 60 optical modules each, so that the neutrino trigger energy threshold can be lowered to a few GeV and thus high-quality reconstructions for neutrino events can be achieved between 5 and 15 GeV. Such a detector geometry will be able to distinguish between the normal and inverted neutrino mass hierarchies at the 3σ significance with an estimated 3.5 years of data taking.

The survival probability of atmospheric muon neutrinos that reach the PINGU detector after propagation through the Earth (i.e., from below) depends on their beam energy E and propagation length L . Thanks to interactions with electrons within the Earth, a resonant flavor conversion can happen at a specific pattern of neutrino energies and Earth-crossing paths. This matter-induced resonant conversion occurs only for neutrinos in the normal mass ordering or only for antineutrinos in the inverted mass ordering, as the behaviors of $\nu_\mu \rightarrow \nu_\mu$ and $\bar{\nu}_\mu \rightarrow \bar{\nu}_\mu$ oscillations depend respectively on $\Delta m_{31}^2 \mp 2\sqrt{2}G_F N_e E$, where N_e is the number density of electrons in matter and E denotes the neutrino beam energy. The PINGU detector is capable of discriminating the cross sections and kinematics of neutrino and antineutrino interactions with nuclei, so it is capable of identifying different detected event rates which depend on different neutrino mass orderings.

Given an accelerator-driven neutrino beam, the long-baseline oscillation experiments are also sensitive to the neutrino mass ordering. Because of the interaction of neutrinos with terrestrial matter as they pass through the Earth, the probability of $\nu_\mu \rightarrow \nu_e$ oscillations can be approximately expressed as⁵⁹

$$\begin{aligned}
 P(\nu_\mu \rightarrow \nu_e) \simeq & \sin^2 2\theta_{13} \sin^2 \theta_{23} \frac{\sin^2(x-1)\Delta_{31}}{(x-1)^2} + \alpha \sin 2\theta_{12} \sin 2\theta_{13} \sin 2\theta_{23} \\
 & \times \cos(\Delta_{31} + \delta) \frac{\sin x \Delta_{31} \sin(x-1)\Delta_{31}}{x(x-1)} \\
 & + \alpha^2 \sin^2 2\theta_{12} \cos^2 \theta_{23} \frac{\sin^2 x \Delta_{31}}{x^2}, \tag{7}
 \end{aligned}$$

where $x \equiv 2\sqrt{2}G_F N_e E / \Delta m_{31}^2$ and $\alpha \equiv \Delta m_{21}^2 / \Delta m_{31}^2$. One may easily obtain the expression of $P(\bar{\nu}_\mu \rightarrow \bar{\nu}_e)$ from Eq. (7) with the replacements $\delta \rightarrow -\delta$ and $x \rightarrow -x$. So the sign of Δm_{31}^2 affects the behaviors of neutrino oscillations via the signs of x and α . That is why the matter-induced resonant conversion can only occur for neutrinos in the normal mass hierarchy ($x > 0$) or for antineutrinos in the inverted mass hierarchy ($x < 0$), similar to the case of atmospheric neutrino or antineutrino oscillations. In practice the baseline length L of an experiment is crucial for its sensitivity to the mass hierarchy. The LBNE experiment⁷⁵ with $L \simeq 1300$ km is therefore expected to be more promising than the T2K experiment⁵⁸ with $L \simeq 295$ km and the NO ν A experiment⁷⁸ with $L \simeq 810$ km in this respect. But the undetermined CP-violating phase δ may in general give rise to some uncertainties associated with a determination of the neutrino mass hierarchy in the long-baseline experiments. In particular, a careful analysis shows that the mass hierarchy sensitivity is most optimistic (or pessimistic) for $\delta \simeq -\pi/2$ in the normal (or inverted) hierarchy case, or for $\delta \simeq +\pi/2$ in the inverted (or normal) hierarchy case.⁷⁵ Regardless of possible values of δ , LBNE in combination with T2K and NO ν A promises to resolve the neutrino mass hierarchy with a significance of more than 3σ by 2030.⁷⁷

In addition, the proposed Hyper-Kamiokande (HK) detector will be a next-generation underground water Cherenkov detector serving as the far detector of the 295 km-baseline neutrino oscillation experiment for the J-PARC neutrino beam.⁷⁹ It is expected to be ten times larger than the SK detector and capable of probing the neutrino mass ordering, resolving the octant of the largest flavor mixing angle θ_{23} and observing leptonic CP violation as well as proton decays and extraterrestrial neutrinos from distant astrophysical sources.

CP violation in the lepton sector may have far-reaching impacts on our understanding of the origin of matter–antimatter asymmetries at both microscales and macroscales. The LBNE and HK experiments, together with other next-generation long-baseline neutrino oscillation experiments, are aiming at a determination of the CP-violating phase δ . The latter can be extracted from comparing between the probabilities of $\nu_\mu \rightarrow \nu_e$ and $\bar{\nu}_\mu \rightarrow \bar{\nu}_e$ oscillations, but it is in general contaminated by terrestrial matter effects. In the leading-order approximation,

$$\mathcal{A}_{\text{CP}} \equiv \frac{P(\nu_\mu \rightarrow \nu_e) - P(\bar{\nu}_\mu \rightarrow \bar{\nu}_e)}{P(\nu_\mu \rightarrow \nu_e) + P(\bar{\nu}_\mu \rightarrow \bar{\nu}_e)} \simeq -\frac{\sin 2\theta_{12} \sin \delta}{\sin \theta_{13} \tan \theta_{23}} \Delta_{21} + \text{matter effects}, \quad (8)$$

where the term of matter effects should more or less be correlated with the neutrino mass ordering. To lower the matter contamination, one may therefore consider a low-energy neutrino (or antineutrino) beam with a much shorter baseline length.⁸⁰ A proposal of this kind is the MOMENT project with a neutrino beam energy $E \sim 300$ MeV and a baseline length $L \sim 120$ km,⁸¹ towards probing leptonic CP violation before a more powerful neutrino factory is built.

6. Two Non-Oscillation Aspects

6.1. Neutrinoless double-beta decays

Soon after Fermi developed an effective beta decay theory,⁵ Maria Goeppert-Mayer pointed out that certain even-even nuclei should have a chance to decay into the second nearest neighbors via two simultaneous beta decays:⁸² $(A, Z) \rightarrow (A, Z+2) + 2e^- + 2\bar{\nu}_e$, where the kinematic conditions $m(A, Z) > m(A, Z+2)$ and $m(A, Z) < m(A, Z+1)$ must be satisfied. In 1939 Wendell Furry further pointed out that the $0\nu\beta\beta$ decays $(A, Z) \rightarrow (A, Z+2) + 2e^-$ could happen via an exchange of the *virtual* neutrinos between two associated beta decays,⁸³ provided the neutrinos are massive and have the Majorana nature.¹⁰ If such a $0\nu\beta\beta$ process is measured, does it definitely imply the existence of a Majorana mass term for neutrinos? The answer is affirmative according to the Schechter–Valle theorem,⁸⁴ no matter whether there are new physics contributions to the $0\nu\beta\beta$ decays. Hence the $0\nu\beta\beta$ transitions can serve for an experimentally feasible probe towards identifying the Majorana nature of massive neutrinos at low energies.

The half-life of a $0\nu\beta\beta$ -decaying nuclide can be expressed as follows:

$$T_{1/2}^{0\nu} = (G^{0\nu})^{-1} |M^{0\nu}|^{-2} |\langle m \rangle_{ee}|^{-2}, \quad \langle m \rangle_{ee} \equiv \sum_i (m_i U_{ei}^2), \quad (9)$$

where $G^{0\nu}$ is the phase-space factor, $M^{0\nu}$ stands for the relevant nuclear matrix element, and $\langle m \rangle_{ee}$ denotes the effective Majorana neutrino mass in the absence of new physics contributions. Among them, the calculation of $|M^{0\nu}|$ relies on the chosen nuclear models which are only able to approximately describe the many-body interactions of nucleons in nuclei, and thus it involves the largest theoretical uncertainty (e.g., a factor of two or three for some typical nuclei).⁸⁵ This causes quite a big uncertainty associated with the determination of $|\langle m \rangle_{ee}|$.

So far no convincing evidence for an occurrence of the $0\nu\beta\beta$ decay has been established, although a lot of experimental efforts have been made in the past few decades. Such an experiment is designed to observe the two electrons emitted in a given $0\nu\beta\beta$ decay, and its signature is based on the fact that the sum of the energies of the two emitted electrons is equal to the Q -value of this process. In contrast, the energy spectrum of the two emitted electrons in a normal double-beta decay must be continuous. At present the strongest upper bound on the effective mass term $|\langle m \rangle_{ee}|$ can be set by the ${}^{76}_{32}\text{Ge} \rightarrow {}^{76}_{34}\text{Se} + 2e^-$ and ${}^{136}_{54}\text{Xe} \rightarrow {}^{136}_{56}\text{Ba} + 2e^-$ experiments.⁸⁵ In particular, the GERDA,⁸⁶ EXO-200⁸⁷ and KamLAND-Zen⁸⁸ experiments have obtained $T_{1/2}^{0\nu} > 2.1 \times 10^{25}$ yr, 1.1×10^{25} yr and 1.9×10^{25} yr at the 90% confidence level, respectively. These results lead to the constraints $|\langle m \rangle_{ee}| < 0.22\text{--}0.64$ eV, $0.2\text{--}0.69$ eV and $0.15\text{--}0.52$ eV at the same confidence level, respectively, after the relevant uncertainties of nuclear matrix elements are taken into account.⁸⁵

The expected magnitude of $|\langle m \rangle_{ee}|$ in the standard three-flavor case is illustrated in Fig. 10, where current neutrino oscillation data have been input and arbitrary values of the CP-violating phases have been taken.⁸⁹ It is clear that the inverted neutrino mass ordering or a near neutrino mass degeneracy may allow $|\langle m \rangle_{ee}| \geq 0.01$ eV, which should be accessible in the next-generation $0\nu\beta\beta$ -decay experiments. If the neutrino mass spectrum is normal and hierarchical, however, there will be little prospect of observing any $0\nu\beta\beta$ decays in the foreseeable future, simply because of $|\langle m \rangle_{ee}| \sim \mathcal{O}(10^{-3})$ eV in this unfortunate case.

6.2. The absolute neutrino mass scale

Since the flavor oscillations of massive neutrinos are only sensitive to the neutrino mass-squared differences, a determination of the absolute neutrino mass scale has to rely on some non-oscillation experiments. Searching for the $0\nu\beta\beta$ decay is one of the feasible ways for this purpose if massive neutrinos are the Majorana particles, because the magnitude of its effective mass term $\langle m \rangle_{ee}$ is associated with m_i as shown in Eq. (9) and Fig. 10. Another way is to detect the beta decays, such as

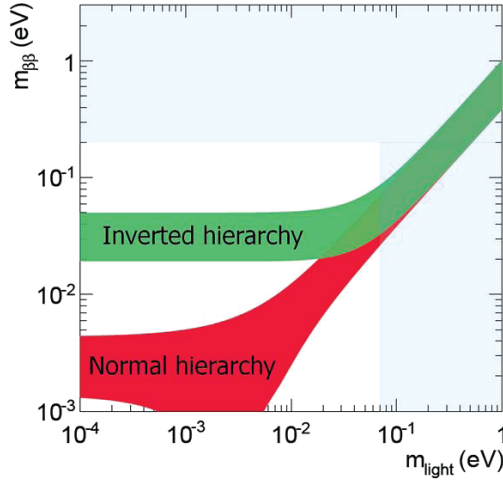


Fig. 10. The effective Majorana neutrino mass $m_{\beta\beta} \equiv |\langle m \rangle_{ee}|$ as a function of the lightest neutrino mass $m_{\text{light}} \equiv m_1$ (normal hierarchy, red band) or m_3 (inverted hierarchy, green band).⁸⁹ Here the horizontally-excluded region comes from the $0\nu\beta\beta$ experiments,^{86–88} and the vertically-excluded region is due to the cosmological bound.⁹⁰

${}^3_1\text{H} \rightarrow {}^3_2\text{He} + e^- + \bar{\nu}_e$, whose effective neutrino mass term $\langle m \rangle_e$ is defined via

$$(\langle m \rangle_e)^2 \equiv \sum_i (m_i^2 |U_{ei}|^2) . \tag{10}$$

The most promising experiment of this kind is the KATRIN experiment,⁹¹ which may hopefully probe $\langle m \rangle_e$ with a sensitivity of about 0.2 eV in the near future. But up to now only $\langle m \rangle_e < 2.05$ eV has been obtained at the 95% confidence level from the Troitzk beta-decay experiment.⁹²

Furthermore, one may get useful information on the mass scale of light neutrinos from cosmology. Based on the standard Λ CDM model, a global analysis of current cosmological data (especially those on the cosmic microwave background (CMB) radiation and large-scale structure (LSS) formation) can provide us with the most powerful sensitivity to the sum of light neutrino masses via the relation

$$\Omega_\nu h^2 = \frac{1}{93 \text{ eV}} \Sigma_\nu, \quad \Sigma_\nu \equiv \sum_i m_i, \tag{11}$$

in which Ω_ν denotes the light neutrino contribution to today’s energy density of the Universe, and h is the Hubble constant. For example, $\Sigma_\nu < 0.23$ eV has recently been reported by the Planck Collaboration at the 95% confidence level.⁹⁰ If a combination of the next-generation CMB and LSS measurements can reach a sensitivity of about 0.02 eV for the sum of three neutrino masses,⁹³ then it will be possible to determine the absolute neutrino mass scale via a definite determination of Σ_ν , even though the neutrino mass ordering is normal.

Note that it is also possible to determine or constrain the absolute neutrino mass scale m_ν through the study of kinematic effects of supernova neutrinos, because their flight time from a supernova's core to a terrestrial detector will be more or less delayed as compared with the massless particles.⁹⁴ A careful analysis of the $\bar{\nu}_e$ events from the Supernova 1987A explosion led us to an upper bound of about 6 eV on m_ν .⁹⁵ The prospects of this astrophysical approach depend on the emergence of new neutrino detectors or the existence of antineutrino pulses in the first instants of a supernova explosion.⁹⁶ Given the JUNO liquid scintillator detector as an example, $m_\nu < 0.83 \pm 0.24$ eV is expected to be achievable at the 95% confidence level for a typical galactic supernova at a distance of 10 kpc from the Earth.⁹⁷

7. Summary and Outlook

Since 1998, quite a lot of significant breakthroughs have been made in experimental neutrino physics. On the one hand, the exciting phenomena of atmospheric, solar, reactor and accelerator neutrino or antineutrino oscillations have all been observed, and the oscillation parameters Δm_{21}^2 , $|\Delta m_{31}^2|$, θ_{12} , θ_{13} and θ_{23} have been determined to an impressive degree of accuracy. On the other hand, the geo-antineutrino events and extraterrestrial PeV neutrino events have been observed, and the sensitivities to neutrino masses in the beta decays, $0\nu\beta\beta$ decays and cosmology have been improved to a great extent. Furthermore, a lot of theoretical efforts have also been made towards understanding the origin of tiny neutrino masses and the flavor structure behind the observed neutrino mixing pattern, and towards studying possible implications of massive neutrinos on the cosmological matter–antimatter asymmetry, warm dark matter and many violent astrophysical processes.^{29,98} All these have demonstrated neutrino physics to be one of the most important frontiers of particle physics, astrophysics and cosmology.

But a number of fundamental questions about massive neutrinos remain open. The burning ones include how small the absolute neutrino mass scale is, whether the neutrino mass spectrum is normal or inverted, whether massive neutrinos are the Majorana particles, how large the CP-violating phase δ is, which octant the largest flavor mixing angle θ_{23} belongs to, whether there are light and (or) heavy sterile neutrinos, what the role of neutrinos is in dark matter, whether the observed matter–antimatter asymmetry of the Universe is related to CP violation in neutrino oscillations, etc. Motivated by so many questions, we are trying to discover a new physics world with the help of massive neutrinos in the coming decades.

Acknowledgments

We would like to thank Luciano Maiani and Gigi Rolandi for inviting us to contribute to this book. We are also grateful to Yu-Feng Li, Jue Zhang, Zhen-hua Zhao, Shun Zhou and Ye-Ling Zhou for their helpful comments on this essay. This

work is supported in part by the National Natural Science Foundation of China under grant No. 11135009 and 11390380; by the National Basic Research Program of China under grant No. 2013CB834300; by the Strategic Priority Research Program of the Chinese Academy of Sciences (CAS) under grant No. XDA10000000; and by the CAS Center for Excellence in Particle Physics.

References

1. A. H. Becquerel, *Compt. Rend. Math.* **122**, 420 (1896).
2. J. Chadwick, *Verhandle. Deut. Phys.* **16**, 383 (1914).
3. C. D. Ellis and W. A. Wooster, *Proc. Roy. Soc. London A* **117**, 109 (1927).
4. W. Pauli, Lecture given in Zürich in 1957, published in *Physik und Erkenntnistheorie* (Friedr. Vieweg, & Sohn, Braunschweig/Wiesbaden, 1984), p. 156.
5. E. Fermi, *La Ricerca Scientifica* **2**, 12 (1933); *Z. Phys.* **88**, 161 (1934).
6. H. A. Bethe and R. F. Bacher, *Rev. Mod. Phys.* **8**, 184 (1936).
7. B. Pontecorvo, Chalk River Lab. Report PD-205 (1946).
8. C. L. Cowan, F. Reines, F. B. Harrison, H. W. Kruse, and A. D. McGuire, *Science* **124**, 103 (1956).
9. B. Pontecorvo, *Sov. Phys. JETP* **6**, 429 (1957).
10. E. Majorana, *Nuovo Cim.* **14**, 171 (1937).
11. G. Danby *et al.*, *Phys. Rev. Lett.* **9**, 36 (1962).
12. Z. Maki, M. Nakagawa, and S. Sakata, *Prog. Theor. Phys.* **28**, 870 (1962).
13. K. Kodama *et al.* (DONUT Collaboration), *Phys. Rev. Lett.* **504**, 218 (2001).
14. J. A. Formaggio and G. P. Zeller, *Rev. Mod. Phys.* **84**, 1307 (2012).
15. S. L. Glashow, *Phys. Rev.* **118**, 316 (1960).
16. S. Weinberg, *Phys. Rev.* **128**, 1457 (1962); J. M. Irvine and R. Humphreys, *J. Phys. G* **9**, 847 (1983); A. Cocco, G. Mangano, and M. Messina, *JCAP* **0706**, 015 (2007); Y. F. Li, Z. Z. Xing, and S. Luo, *Phys. Lett. B* **692**, 261 (2010).
17. S. Betts *et al.*, arXiv:1307.4738 (2013).
18. T. Araki *et al.* (KamLAND Collaboration), *Nature* **436**, 499 (2005); S. Abe *et al.* (KamLAND Collaboration), *Phys. Rev. Lett.* **100**, 221803 (2008).
19. G. Bellini *et al.* (Borexino Collaboration), *Phys. Lett. B* **687**, 299 (2010).
20. H. A. Bethe, *Phys. Rev.* **55**, 434 (1939); G. Gamow and M. Schönberg, *Phys. Rev.* **58**, 1117 (1940); *Phys. Rev.* **59**, 539 (1941).
21. R. Davis, D. S. Harmer, and K. C. Hoffman, *Phys. Rev. Lett.* **20**, 1205 (1968); J. N. Bahcall and G. Shaviv, *Phys. Rev. Lett.* **20**, 1209 (1968).
22. H. A. Bethe and J. R. Wilson, *Astrophys. J.* **295**, 14 (1985); H. A. Bethe, *Rev. Mod. Phys.* **62**, 801 (1990).
23. K. Hirata *et al.* (Kamiokande Collaboration), *Phys. Rev. Lett.* **58**, 1490 (1987).
24. R. M. Bionta *et al.* (IMB Collaboration), *Phys. Rev. Lett.* **58**, 1494 (1987).
25. E. N. Alekseev *et al.*, *JETP Lett.* **45**, 589 (1987).
26. K. A. Olive *et al.* (Particle Data Group), *Chin. Phys. C* **38**, 090001 (2014).
27. Y. Fukuda *et al.* (Super-Kamiokande Collaboration), *Phys. Rev. Lett.* **81**, 1562 (1998).
28. M. G. Aartsen *et al.* (IceCube Collaboration), *Science* **342**, 1242856 (2013); *Phys. Rev. Lett.* **113**, 101101 (2014).
29. Z. Z. Xing and S. Zhou, *Neutrinos in Particle Physics, Astronomy and Cosmology* (Zhejiang University Press and Springer-Verlag, 2011).
30. L. Wolfenstein, *Phys. Rev. D* **17**, 2369 (1978); S. P. Mikheyev and A. Yu. Smirnov, *Sov. J. Nucl. Phys.* **42**, 913 (1985).

31. F. J. Hasert *et al.*, *Phys. Lett. B* **46**, 138 (1973).
32. S. L. Glashow, *Nucl. Phys.* **22**, 579 (1961); S. Weinberg, *Phys. Rev. Lett.* **19**, 1264 (1967); A. Salam, in *Elementary Particle Physics (Nobel Symposium No. 8)*, edited by N. Svartholm (Almqvist and Wilsell, 1968), p. 367.
33. Arnison *et al.* (UA1 Collaboration), *Phys. Lett. B* **122**, 103 (1983); *Phys. Lett. B* **126**, 398 (1983).
34. Z. Z. Xing, *Prog. Theor. Phys. Suppl.* **180**, 112 (2009).
35. S. Weinberg, *Phys. Rev. Lett.* **43**, 1566 (1979).
36. P. Minkowski, *Phys. Lett. B* **67**, 421 (1977); T. Yanagida, in *Proceedings of the Workshop on Unified Theory and the Baryon Number of the Universe*, edited by O. Sawada and A. Sugamoto (KEK, Tsukuba, 1979), p. 95; M. Gell-Mann, P. Ramond, and R. Slansky, in *Supergravity*, edited by P. van Nieuwenhuizen and D. Freedman (North Holland, Amsterdam, 1979), p. 315; S. L. Glashow, in *Quarks and Leptons*, edited by M. Lévy *et al.* (Plenum, New York, 1980), p. 707; R. N. Mohapatra and G. Senjanovic, *Phys. Rev. Lett.* **44**, 912 (1980).
37. M. Fukugita and T. Yanagida, *Phys. Lett. B* **174**, 45 (1986).
38. W. J. Marciano and A. I. Sanda, *Phys. Lett. B* **67**, 303 (1977); B. W. Lee and R. Shrock, *Phys. Rev. D* **16**, 1444 (1977); K. Fujikawa and R. Shrock, *Phys. Rev. Lett.* **45**, 963 (1980); R. Shrock, *Nucl. Phys. B* **206**, 359 (1982); P. Pal and L. Wolfenstein, *Phys. Rev. D* **25**, 766 (1982).
39. For a review, see: C. Giunti and A. Studenikin, *Phys. Atom. Nucl.* **72**, 2089 (2009).
40. S. Antusch, C. Biggio, E. Fernandez-Martinez, M. B. Gavela, and J. Lopez-Pavon, *JHEP* **0610**, 084 (2006); S. Antusch and O. Fischer, *JHEP* **1410**, 94 (2014).
41. J. Schechter and J. W. F. Valle, *Phys. Rev. D* **23**, 1666 (1981); Z. Z. Xing, *Phys. Rev. D* **87**, 053019 (2013); Z. Z. Xing and Y. L. Zhou, *Phys. Rev. D* **88**, 033002 (2013).
42. J. N. Bahcall, *Phys. Rev. Lett.* **12**, 300 (1964).
43. B. T. Cleveland *et al.* (Homestake Collaboration), *Astrophys. J.* **496**, 505 (1998).
44. W. Hampel *et al.* (GALLEX Collaboration), *Phys. Lett. B* **447**, 127 (1999); M. Altmann *et al.* (GNO Collaboration), *Phys. Lett. B* **490**, 16 (2000).
45. J. N. Abdurashitov *et al.* (SAGE Collaboration), *JETP* **95**, 181 (2002).
46. Y. Fukuda *et al.* (Super-Kamiokande Collaboration), *Phys. Rev. Lett.* **81**, 1158 (1998).
47. Q. R. Ahmad *et al.* (SNO Collaboration), *Phys. Rev. Lett.* **89**, 011301 (2002).
48. B. Aharmim *et al.* (SNO Collaboration), *Phys. Rev. C* **72**, 055502 (2005).
49. B. Kayser, arXiv:0804.1497 (2008).
50. C. Arpesella *et al.* (Borexino Collaboration), *Phys. Lett. B* **658**, 101 (2008); *Phys. Rev. Lett.* **101**, 091302 (2008).
51. K. S. Hirata *et al.* (Kamiokande-II Collaboration), *Phys. Lett. B* **205**, 416 (1988); *Phys. Lett. B* **280**, 146 (1992).
52. D. Casper *et al.*, *Phys. Rev. Lett.* **66**, 2561 (1991); R. Becker-Szendy *et al.*, *Phys. Rev. D* **46**, 3720 (1992).
53. Y. Ashie *et al.* (Super-Kamiokande Collaboration), *Phys. Rev. Lett.* **93**, 101801 (2004).
54. K. Abe *et al.* (Super-Kamiokande Collaboration), *Phys. Rev. Lett.* **110**, 181802 (2013).
55. M. H. Ahn *et al.* (K2K Collaboration), *Phys. Rev. Lett.* **90**, 041801 (2003).
56. D. Michael *et al.* (MINOS Collaboration), *Phys. Rev. Lett.* **97**, 191801 (2006).
57. A. Strumia and F. Vissani, arXiv:hep-ph/0606054 (2006).
58. K. Abe *et al.* (T2K Collaboration), *Phys. Rev. Lett.* **107**, 041801 (2011); *Phys. Rev. Lett.* **111**, 211803 (2013); *Phys. Rev. Lett.* **112**, 061802 (2014); *Phys. Rev. Lett.* **112**, 181801 (2014).
59. See, e.g., M. Freund, *Phys. Rev. D* **64**, 053003 (2001).
60. N. Agafonova *et al.* (OPERA Collaboration), *PTEP* **2014**, 101C01 (2014).

61. K. Eguchi *et al.* (KamLAND Collaboration), *Phys. Rev. Lett.* **90**, 021802 (2003).
62. F. P. An *et al.* (Daya Bay Collaboration), *Phys. Rev. Lett.* **108**, 171803 (2012); *Chin. Phys. C* **37**, 011001 (2013).
63. S. Abe *et al.* (KamLAND Collaboration), *Phys. Rev. Lett.* **100**, 221803 (2008).
64. M. Apollonio *et al.* (CHOOZ Collaboration), *Phys. Lett. B* **420**, 397 (1998).
65. F. Boehm *et al.* (Palo Verde Collaboration), *Phys. Rev. Lett.* **84**, 3764 (2000).
66. J. K. Ahn *et al.* (RENO Collaboration), *Phys. Rev. Lett.* **108**, 191802 (2012).
67. Y. Abe *et al.* (Double Chooz Collaboration), *Phys. Rev. D* **86**, 052008 (2012); *Phys. Lett. B* **723**, 66 (2013).
68. F. P. An *et al.* (Daya Bay Collaboration), *Phys. Rev. Lett.* **112**, 061801 (2014).
69. F. Capozzi, G. L. Fogli, E. Lisi, A. Marrone, D. Montanino, and A. Palazzo, *Phys. Rev. D* **89**, 093018 (2014).
70. D. V. Forero, M. Tortola, and J. W. F. Valle, *Phys. Rev. D* **90**, 093006 (2014).
71. M. C. Gonzalez-Garcia, M. Maltoni, and T. Schwetz, *JHEP* **1411**, 052 (2014).
72. Z. Z. Xing and S. Zhou, *Phys. Lett. B* **666**, 166 (2008).
73. Y. F. Li, J. Cao, Y. Wang, and L. Zhan, *Phys. Rev. D* **88**, 013008 (2013).
74. M. G. Aartsen *et al.* (IceCube-PINGU Collaboration), arXiv:1401.2046 (2014).
75. C. Adams *et al.* (LBNE Collaboration), arXiv:1307.7335 (2013).
76. L. Zhan, Y. Wang, J. Cao, and L. Wen, *Phys. Rev. D* **78**, 111103 (2008); *Phys. Rev. D* **79**, 073007 (2009).
77. R. N. Cahn *et al.*, arXiv:1307.5487 (2013).
78. D. S. Ayres *et al.* (NO ν A Collaboration), arXiv:hep-ex/0503053 (2005).
79. K. Abe *et al.* (Hyper-Kamiokande Working Group), arXiv:1109.3262 (2011).
80. See, e.g., M. Koike and J. Sato, *Phys. Rev. D* **61**, 073012 (2000); H. Minakata and H. Nunokawa, *Phys. Lett. B* **495**, 369 (2000).
81. J. Cao *et al.*, *Phys. Rev. S. T. A. B.* **17**, 090101 (2014).
82. M. Goeppert-Mayer, *Phys. Rev.* **48**, 512 (1935).
83. W. H. Furry, *Phys. Rev.* **56**, 1184 (1939).
84. J. Schechter and J. W. F. Valle, *Phys. Rev. D* **25**, 2951 (1982).
85. S. M. Bilenky and C. Giunti, *Int. J. Mod. Phys. A* **30**, 1530001 (2015).
86. M. Agostini *et al.* (GERDA Collaboration), *Phys. Rev. Lett.* **111**, 122503 (2013).
87. J. Albert *et al.* (EXO-200 Collaboration), *Nature* **510**, 229 (2014).
88. A. Gando *et al.* (KamLAND-Zen Collaboration), *Phys. Rev. Lett.* **110**, 062502 (2013).
89. J. J. Gomez-Cadenas and J. Martin-Albo, arXiv:1502.00581 (2015).
90. P. A. R. Ade *et al.* (Planck Collaboration), *Astron. Astrophys.* **571**, A16 (2014).
91. L. Bornschein *et al.* (KATRIN Collaboration), hep-ex/0309007 (2003).
92. V. N. Aseev *et al.*, *Phys. Rev. D* **84**, 112003 (2011).
93. K. N. Abazajian *et al.*, *Astropart. Phys.* **63**, 66 (2015).
94. G. T. Zatsepin, *Pisma Zh. Eksp. Teor. Fiz.* **8**, 333 (1968).
95. T. J. Loredo and D. Q. Lamb, *Phys. Rev. D* **65**, 063002 (2002); G. Pagliaroli, F. Rossi-Torres, and F. Vissani, *Astropart. Phys.* **33**, 287 (2010).
96. S. Dell’Oro, S. Marcocci, and F. Vissani, *Phys. Rev. D* **90**, 033005 (2014).
97. J. S. Lu, J. Cao, Y. F. Li, and S. Zhou, arXiv:1412.7418 (2014).
98. See, e.g., H. Fritzsch and Z. Z. Xing, *Prog. Part. Nucl. Phys.* **45**, 1 (2000); Z. Z. Xing, *Int. J. Mod. Phys. A* **19**, 1 (2004); G. Altarelli and F. Feruglio, *Rev. Mod. Phys.* **82**, 2701 (2010); S. F. King and C. Luhn, *Rept. Prog. Phys.* **76**, 056201 (2013).